The Forkhead Box m1 Transcription Factor Stimulates the Proliferation of Tumor Cells during Development of Lung Cancer

Il-Man Kim,[1,3] Timothy Ackerson,[3] Sneha Ramakrishna,[1] Maria Tretiakova,[2] I-Ching Wang,[3] Tanya V. Kalin,[1] Michael L. Major,[3] Galina A. Gusarova,[3] Helena M. Yoder,[3] Robert H. Costa,[3] and Vladimir V. Kalinichenko[1]

Departments of [1]Medicine and [2]Pathology, University of Chicago, Chicago, Illinois; and [3]Department of Biochemistry and Molecular Genetics, University of Illinois at Chicago, Chicago, Illinois

Abstract

The proliferation-specific Forkhead Box m1 (Foxm1 or Foxm1b) transcription factor (previously called HFH-11B, Trident, Win, or MPP2) regulates expression of cell cycle genes essential for progression into DNA replication and mitosis. Expression of Foxm1 is found in a variety of distinct human cancers including hepatocellular carcinomas, intrahepatic cholangiocarcinomas, basal cell carcinomas, ductal breast carcinomas, and anaplastic astrocytomas and glioblastomas. In this study, we show that human Foxm1 protein is abundantly expressed in highly proliferative human non–small cell lung cancers (NSCLC) as well as in mouse lung tumors induced by urethane. To determine the role of Foxm1 during the development of mouse lung tumors, we used IFN-inducible Mx-Cre recombinase transgene to delete mouse *Foxm1* fl/fl–targeted allele before inducing lung tumors with urethane. We show that Mx-Cre *Foxm1*$^{-/-}$ mice exhibit diminished proliferation of lung tumor cells causing a significant reduction in number and size of lung adenomas. Transient transfection experiments with A549 lung adenocarcinoma cells show that depletion of Foxm1 levels by short interfering RNA caused diminished DNA replication and mitosis and reduced anchorage-independent growth of cell colonies on soft agar. Foxm1-depleted A549 cells exhibit reduced expression of cell cycle–promoting *cyclin A2* and *cyclin B1* genes. These data show that Foxm1 stimulates the proliferation of tumor cells during progression of NSCLC. (Cancer Res 2006; 66(4): 2153-61)

Introduction

Lung cancer is the leading cause of cancer-related death in men and women in the United States (1). Human lung cancers are subdivided into small cell lung cancer (SCLC) and non–small cell lung cancer (NSCLC), the latter of which consists of squamous, adenocarcinoma, and large cell carcinoma. Development of cancer is a multistep process involving the gain of function mutations that activate the cell cycle–promoting Ras/mitogen-activated protein kinase (MAPK) signaling pathway (2), as well as the loss of function mutations of tumor suppressor genes (3). Activating mutations in K-Ras oncogene occur in the majority of spontaneous and chemically induced mouse lung tumors (4), as well as in a subset of human NSCLC (5). Fifty percent of NSCLC tumors contain mutations of the p53 tumor suppressor gene, whereas 30% of NSCLC tumors express high levels of the c-*myc* protein (6). Inactivation of $p19^{ARF}$ and $p16^{INK}$ tumor suppressor genes due to promoter silencing is frequently associated with NSCLC (3). Adenocarcinoma is the most common type of lung cancer, which exhibits metastases before clinical symptoms become apparent, thus reducing successful treatment options. Therefore, identification of new molecular targets, which are essential for proliferation of tumor cells, will benefit both treatment and chemoprevention of NSCLC.

Activation of the Ras/MAPK signaling pathway drives cell cycle progression by temporal expression of cyclin regulatory subunits, which activate their corresponding cyclin-dependent kinases (cdk) through complex formation and then phosphorylate target proteins essential for cell cycle progression (2, 3). One of these cdk/cyclin targets is the proliferation-specific Forkhead Box m1 (Foxm1) transcription factor (previously known as HFH-11B, Trident, Win, or MPP2), which recruits cdk/cyclin complexes to the Foxm1 activation domain, where they phosphorylate and stimulate Foxm1 transcriptional activity (7). Activated MAPK (extracellular signal-regulated kinase) kinase has been recently shown to directly phosphorylate the Foxm1 protein, contributing to its transcriptional activation (8). Foxm1 is known to stimulate the transcription of genes essential for progression into DNA replication and mitosis (9). The Foxm1 protein decreases nuclear levels of the CDK inhibitor proteins $p27^{kip1}$ and $p21^{cip1}$ (10–12), which promote cell cycle arrest by inhibiting activation of the cdk2/cyclin complexes. *Foxm1*$^{-/-}$ mice exhibit embryonic lethality due to severe abnormalities in development of the heart, liver, and lung (13, 14). This is caused by a failure to complete mitosis causing a significant reduction in the number of cells in these developing mouse organs. This process was associated with diminished protein levels of Polo-like kinase 1 and Aurora B kinase (13, 14), both of which phosphorylate proteins essential for orchestrating mitosis and cytokinesis (15, 16). Furthermore, we previously reported on generating transgenic mice, in which the Rosa26 promoter drives ubiquitous expression of the Foxm1 transgene, and showed that the Foxm1 stimulates proliferation of all lung cell types in response to butylated hydroxytoluene (BHT) lung injury (17).

Consistent with the important role of Foxm1 in cell cycle progression, elevated Foxm1 levels are found in numerous cell lines derived from tumors (18–20). Increased expression of Foxm1 was also found in human basal cell carcinomas (21), intrahepatic

Requests for reprints: Vladimir V. Kalinichenko, Department of Medicine, Section of Pulmonary and Critical Care Medicine, The University of Chicago, Room W661, MC 6076, 5841 South Maryland Avenue, Chicago, IL 60637. Phone: 773-702-4024; Fax: 773-702-6500; E-mail: vkalin@medicine.bsd.uchicago.edu.

doi:10.1158/0008-5472.CAN-05-3003

cholangiocarcinomas (22), anaplastic astrocytomas and glioblastomas (23), infiltrating ductal breast carcinomas (24), and in many other solid tumors (25). This suggests that Foxm1 is required for cellular proliferation in various human cancers. Foxm1 is also overexpressed in hepatocellular carcinomas from patients that respond poorly to treatment (26). We recently showed that Alb-Cre *Foxm1* fl/fl hepatocytes are highly resistant to developing hepatocellular carcinoma following diethylnitrosamine/phenobarbital liver tumor induction, and Foxm1 is a novel inhibitory target of the $p19^{ARF}$ tumor suppressor protein (12). The mechanism of resistance to hepatocellular carcinoma development is associated with defects in cellular proliferation due to an aberrant increase in hepatocyte nuclear levels of cdk inhibitor $p27^{Kip1}$ protein and diminished expression of the M-phase promoting Cdc25B phosphatase (12). Although the Foxm1 protein is essential for hepatocyte proliferation during progression of hepatocellular carcinoma (12), the role of Foxm1 in lung cancer remains to be determined. In this article, we showed that Foxm1 is abundantly expressed in highly proliferative human NSCLC. Conditional deletion of mouse *Foxm1* fl/fl–targeted allele caused a significant reduction in the proliferation of lung tumor cells as well as in the number and size of lung adenomas following the urethane lung tumor induction. Depletion of Foxm1 levels in A549 lung cancer cell line by short interfering RNA (siRNA) transfection caused diminished DNA replication and mitosis, decreased expression of cell cycle promoting *cyclin A2* and *cyclin B1* genes, and reduced anchorage-independent growth of cell colonies on soft agar. These data show that Foxm1 stimulates the proliferation of lung tumor cells during progression of NSCLC.

Materials and Methods

***Foxm1* fl/fl mice and the lung tumorigenesis protocol.** We previously described the generation of the *Foxm1* fl/fl mice, which were bred for five generations into the C57BL/6 mouse genetic background (13). The *Foxm1* fl/fl mice were then bred for two generations with Mx-Cre C57BL/6 transgenic mice to generate Mx-Cre *Foxm1* fl/fl mice. *Foxm1* fl/fl (control) and Mx-Cre *Foxm1* fl/fl (experimental; Mx-Cre $Foxm1^{-/-}$) 8- to 12-week-old male mice were i.p. injected three times with 250 μL of synthetic double-stranded RNA (dsRNA; also known as PolyI:PolyC or PIPC; 1.25 mg/mL in PBS) during a period of 1 week to induce IFN-α/β production *in vivo* and subsequent activation of Mx-Cre transgene as described previously (27). An additional group of Mx-Cre *Foxm1* fl/fl mice was injected with PBS instead of dsRNA to use as a second control. Using this protocol, the deletion of *Foxm1* fl/fl–targeted allele was induced in all cell types producing the $Foxm1^{-/-}$ allele, which lacks the DNA binding and transcriptional activation domains (13, 27).

One week after the last dsRNA treatment, the mice were i.p. injected with 1 g/kg of urethane (Sigma, St. Louis, MO) once a week for 10 consecutive weeks to achieve 100% incidence of lung tumors in C57BL/6 mouse background (28). Mice were sacrificed at 28 weeks following the initial urethane injection and examined for lung tumors using a dissecting microscope. Lung tissues were then used for preparation of total lung RNA or fixed, paraffin embedded, sectioned, and stained with H&E for morphologic examination.

Bromodeoxyuridine labeling and immunohistochemical staining. To monitor the proliferation of tumor cells, mice were placed on drinking water with 1 mg/mL of bromodeoxyuridine (BrdUrd) for 4 days before they were sacrificed (29). Proliferation rates were detected by immunohistochemistry of mouse lung paraffin sections and the Custom Non–Small Cell Lung Carcinoma TMA human tissue array (US Biomax, Inc., Rockville, MD) using mouse monoclonal antibodies specific for BrdUrd (1:100; clone Bu 20A; DAKO, Carpinteria, CA) or proliferating cell nuclear antigen (PCNA; 1:1,000; clone PC-10; Roche Diagnostics, Indianapolis, IN). Antibody/antigen complexes were detected by anti-mouse antibody conjugated with alkaline phosphatase and 5-bromo-4-chloro-3-indolyl phosphate/nitroblue tetrazolium substrate (all from Vector Labs, Burlingame, CA) as described (30). Lung sections were counterstained with nuclear fast red (Vector Labs). In each mouse lung, we counted the number of BrdUrd-positive cells per 1,000 tumor cells in 10 distinct Foxm1-positive or Foxm1-negative lung tumors in dsRNA-treated Mx-Cre $Foxm1^{-/-}$ mice. Tumors from dsRNA-treated *Foxm1* fl/fl and PBS-treated Mx-Cre *Foxm1* fl/fl mice were used as controls.

We also used rabbit polyclonal antibodies specific to Foxm1 (1:50; ref. 12) and mouse monoclonal antibodies against Foxa2 (1:5; clone 4C7; ref. 14). Antibody/antigen complexes were detected by secondary antibody conjugated with biotin, avidin/horseradish peroxidase (HRP) complex, and 3,3′-diaminobenzidine substrate (all from Vector Labs) as described previously (14).

Western blot analysis. Total protein extracts were prepared from human adenocarcinoma or normal lung tissue and then subjected to Western blot analysis (31) using rabbit polyclonal antibody against Foxm1 (ref. 12; 1:5,000 dilution). We also used mouse monoclonal β-actin antibody (clone AC-15; Sigma; 1:20,000 dilution). Detection of the immune complex was accomplished by using secondary antibodies directly conjugated with HRP followed by chemiluminescence (Supersignal, Pierce, Rockford, IL).

The cancer profiling array. To compare Foxm1 expression in human tumors and corresponding normal tissues, we used the Cancer Profiling Array (Clontech Lab, Palo Alto, CA), which consisted of 241 cDNA pairs derived from normal and tumor tissues of individual patients, including 20 cases with NSCLC. Radioactively labeled cDNA probes were synthesized from human Foxm1 or ubiquitin control cDNA using random primer labeling followed by probe purification on CHROMA SPIN+STE-100 columns (Clontech Lab). Hybridization of the Cancer Profiling Array with human Foxm1 probes and washings of the array were done according to the manufacturer's recommendations (Clontech Lab). The hybridized Cancer Profiling Arrays were then exposed to the phosphorimaging screens and scanned with a Storm 840 PhosphorImager. We then stripped this same membrane and hybridized it with human ubiquitin cDNA probe. Following subtraction of background, Foxm1 hybridization signals were normalized to ubiquitin using IGMac v1.2 program.

siRNA transfection and soft agar assay. To inhibit Foxm1 expression in lung tumor cells in cell culture experiments, we used a 21-nucleotide siRNA duplex specific to 1066-1084 nucleotide region of the human Foxm1 cDNA (siFoxm1, 5′-GGACCACUUUCCCUACUUU-3′). Foxm1 siRNA containing symmetrical 2-Uracil (U) 3′ overhangs was designed and synthesized using Dharmacon Research algorithm. We transfected 100 nmol/L of either siFoxm1 or mutant control siFoxm1 (mutFoxm1; 5′-GGACCUGUAUGCGUACAUU-3′) duplexes into A549 adenocarcinoma cells using LipofectAMINE 2000 reagent (Invitrogen, San Diego, CA) in serum-free tissue culture media following the manufacturer's protocol. A549 cells were harvested at 72 hours after transfection for total RNA preparation or immunofluorescent staining. A549 cells were labeled with BrdUrd for 2 hours and then fixed with ethanol and immunostained for BrdUrd incorporation using the BrdUrd-Labeling and Detection kit I (Roche Diagnostics) according to manufacturer's recommendations.

For soft agar assays, A549 cells were left untransfected or transfected with 100 nmol/L of either siFoxm1 or mutFoxm1. One day after transfection, the cells were trypsinized and plated on soft agar for 2 weeks to assay for anchorage-independent cell growth as described previously (12). Triplicate plates were used to count colonies and determine the mean number of colonies ± SD.

Semiquantitative reverse transcriptase-PCR and RNase protection assay. RNA-STAT-60 (Tel-Test "B," Inc., Friendswood, TX) was used to prepare total RNA from mouse lungs, cultured A549 cells, or human tumor and normal lung tissues, which were obtained from tissue bank of the University of Chicago. After digestion of RNA with DNase I, reverse transcriptase-PCR (RT-PCR) analysis was done as described (32). The following sense and antisense primers were used for amplification: mouse

Foxm1, 5′-GGATCCTGCCACCCCAGACCTTGTTC and 5′-GTCGACTCCCTGATGCTTTTCGCTGTC; mouse cyclophilin, 5′-AGCTCTGAGCACTGGAGAGAAA and 5′-TCCTGAGCTACAGAAGGAATGG; human Foxm1, 5′-GGTCTCGGAGGAAACAGCATCTAC and 5′-TGAAATCCAGTCCCCCTACTTTG; human cyclin B1, 5′-TGTGGATGCAGAAGATGGAT and 5′-AAACATGGCAGTGACACCAA; human cyclophilin, 5′-CTCCTTTGAGCTGTTTGCAG and 5′-CACCACATGCTTGCCATCC. Two different cDNA concentrations were used for RT-PCR reactions to ensure that RT-PCR conditions were in the linear range. Quantitation of expression levels was determined with Tiff files of ethidium bromide–stained gels by using the BioMax 1D program (Kodak, Rochester, NY) as described (32).

RNase protection assay was done with ^{32}P-UTP labeled antisense RNA synthesized from hCYC-1 template (BD Biosciences, San Diego, CA) as described previously (17). Quantitation of expression levels was determined from phosphorimager scans using the ImageQuant program (Amersham Biosciences, Corp., Piscataway, NJ). The ribosomal protein L32 and glyceraldehyde-3-phosphate dehydrogenase hybridization signals were used for normalization control between different RNA samples.

Real-time RT-PCR. Total RNA was digested with RNase-free DNaseI to remove genomic DNA. The Bio-Rad cDNA Synthesis kit containing both oligo-dT and random hexamer primers was used to synthesize cDNA from 10 μg of total RNA. The following reaction mixture was used for all PCR samples: 1× of IQ SybrGreen Supermix (Bio-Rad, Hercules, CA), 100 to 200 nmol/L of each primer, and 2.5 μL of cDNA in a 25 μL total volume. The following sense and antisense primers and annealing temperature (T_a) were used to amplify and measure the amount of mRNA by real-time RT-PCR: human Foxm1, 5′-GGAGGAAATGCCACACTTAGCG and 5′-TAGGACTTCTTGGGTCTTGGGGTG (T_a = 55.7°C); human cyclophilin, 5′-GCAGACAAGGTCCCAAAGACAG and 5′-CACCCTGACACATAAACCCTGG (T_a = 55.7°C); mouse Foxm1, 5′-CACTTGGATTGAGGACCACTT and 5′-GTCGTTTCTGCTGTGATTCC (T_a = 57.5°C); mouse cyclophilin, 5′-GGCAAATGCTGGACCAAACAC and 5′-TTCCTGGACCCAAAACGCTC (T_a = 57.5°C). Reactions were amplified and analyzed in triplicate using a MyiQ Single Color Real-time PCR Detection System (Bio-Rad).

Statistical analysis. Student's t test was used to determine statistical significance. Ps ≤ 0.05 were considered significant. Values for all measurements were expressed as the mean ± SD.

Results

Foxm1 protein is overexpressed in highly proliferative human lung carcinomas. Because Foxm1 is induced in a variety of distinct human carcinoma tumors (21–25), we examined whether Foxm1 is also expressed in human lung carcinomas. We used the Cancer Profiling Array, which consists of cDNA samples derived from 20 human NSCLCs and corresponding adjacent normal lung tissues. Radioactively labeled cDNA probes were synthesized from human Foxm1 or ubiquitin control cDNA and hybridized sequentially with the Cancer Profiling Array (Fig. 1*A*). Following subtraction of background, Foxm1 hybridization signals were normalized to ubiquitin and calculated as a ratio between tumor sample and corresponding normal tissue from the same patient. These results showed that Foxm1 expression is increased >2-fold in 67% (8 of 12 cases) of squamous cell carcinoma and in 50% (4 of 8 cases) of adenocarcinoma of the lung (Fig. 1*B*). Increased levels of Foxm1 mRNA were confirmed in three human NSCLC by quantitative real-time RT-PCR analysis using primers specific for the *Foxm1* gene (Fig. 2*A*).

We next used immunostaining of human NSCLC tissue microarray to compare expression of Foxm1 protein in 56 cases of human lung adenocarcinomas and squamous cell carcinomas with adjacent normal lung tissue from the same patient. Foxm1 protein levels were increased in 72% (13 of 18 cases) of adenocarcinoma specimens and in 68% (17 of 25 cases) of squamous cell carcinoma compared with corresponding normal lung tissue (Fig. 1*C*). These experiments showed that Foxm1 expression is induced in a significant percentage of human lung adenocarcinomas and squamous cell carcinoma tissue samples. Consistent with these results, Western blot analysis showed that total levels of Foxm1 protein were induced in human adenocarcinoma compared with normal lung tissue (Fig. 2*C*).

To determine whether Foxm1 expression correlates with proliferation rates in these human lung tumors, we immunostained an adjacent paraffin section of the same human NSCLC tissue microarray with a mouse monoclonal antibody specific to the PCNA. Our data showed that human lung adenocarcinomas and squamous cell carcinomas expressing high levels of Foxm1 protein exhibited abundant PCNA staining (Fig. 1*D*). Furthermore, increased Foxm1 expression in human lung adenocarcinomas was associated with elevated levels of the cell cycle–promoting cyclin A2 and cyclin B1 as determined by RNase protection assay (Fig. 2*B*). These results show that Foxm1 expression is induced in human NSCLC undergoing rapid proliferation, suggesting that the Foxm1 is involved in stimulating proliferation of lung tumor cells.

Conditional deletion of the *Foxm1* fl/fl allele decreases the total number and size of lung tumors induced by the carcinogen urethane. To determine the role of Foxm1 in mouse lung tumorigenesis, we used the IFN-α/β inducible Mx-Cre recombinase transgene (27) to conditionally delete the *Foxm1* fl/fl–targeted allele before the urethane-mediated lung tumor induction. Expression of the Mx-Cre transgene was induced by three consecutive i.p. injections of mice every other day with synthetic dsRNA PolyI:PolyC or PIPC (27). Eight- to 12-week-old *Foxm1* fl/fl (control) and Mx-Cre *Foxm1* fl/fl male mice (experimental) were induced to delete the *Foxm1* fl/fl–targeted allele, and then 1 week later, they were subjected to weekly i.p. injections of urethane for 10 consecutive weeks to induce formation of lung tumors in C57BL/6 mouse background (28). Based on published studies (28), we sacrificed six control *Foxm1* fl/fl mice and six experimental dsRNA-treated Mx-Cre *Foxm1* fl/fl mice (Mx-Cre *Foxm1*$^{-/-}$) at 28 weeks after initial urethane injection. Another group of Mx-Cre *Foxm1* fl/fl mice were injected with PBS instead of dsRNA to provide information about nonspecific activation of the Mx-Cre transgene due to the secretion of endogenous IFN-α/β. Lungs were dissected and examined for lung tumors using dissecting microscope and then fixed and paraffin embedded. To address the efficiency in deletion of *Foxm1* fl/fl allele, we examined Foxm1 levels in total lung RNA prepared from the left lung lobe using both semiquantitative RT-PCR analysis (Fig. 3*A*) and quantitative real-time RT-PCR (Fig. 3*B*) using two different sets of primers specific for the *Foxm1* gene. Both methods showed ~75% decrease of Foxm1 pulmonary levels in dsRNA-treated Mx-Cre *Foxm1*$^{-/-}$ mice compared with either dsRNA-treated *Foxm1* fl/fl mice or Mx-Cre *Foxm1* fl/fl mice treated with PBS (Fig. 3*A-B*).

Histologic examination of H&E-stained sections revealed that all tumors in *Foxm1* fl/fl or dsRNA-treated Mx-Cre *Foxm1*$^{-/-}$ lungs displayed morphologic characteristics of lungs adenomas (Fig. 4*A*). These lung tumors were epithelial in origin as shown by nuclear staining for Foxa2 protein (Fig. 4*A*), a known marker for alveolar type II cells and bronchial epithelial cells (33). dsRNA-treated Mx-Cre *Foxm1*$^{-/-}$ mice displayed a statistically significant reduction in the total number and diameter of lung adenomas

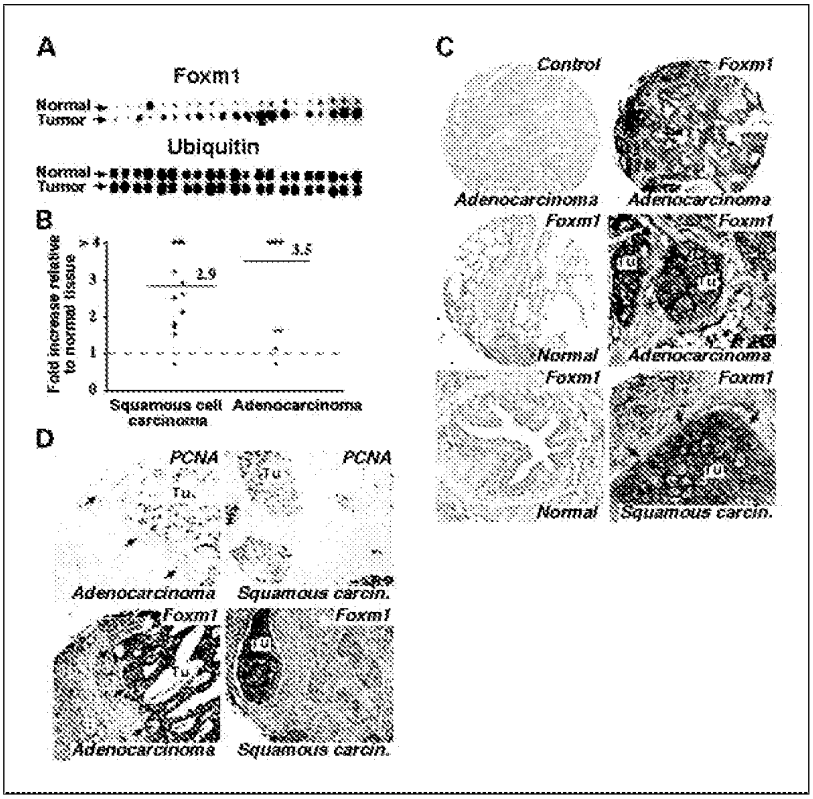

Figure 1. Foxm1 is expressed in the subset of human NSCLC. *A-B,* Cancer Profiling Array shows increased Foxm1 levels in subset of human NSCLCs. The Cancer Profiling Array (Clontech Lab) was used to compare Foxm1 expression in human NSCLC (tumor) and corresponding normal tissues (normal). Radioactively labeled cDNA probes were synthesized from human Foxm1 or ubiquitin control cDNA and hybridized sequentially to the same array membrane. *A,* microphotographs of Foxm1 (*top*) and ubiquitin hybridization signals (*bottom*) from human NSCLC. Foxm1 hybridization signals were normalized to ubiquitin and calculated as a ratio between tumor sample and corresponding normal lung tissue from the same patient. *B,* these relative Foxm1 levels are presented separately for squamous cell carcinoma and adenocarcinoma of the lung. *C,* Foxm1 protein is expressed in a subset of human NSCLC. The Custom Non–Small-Cell Lung Carcinoma TMA tissue arrays from Biomax were stained with rabbit polyclonal Foxm1 antibody followed by anti-rabbit antibody conjugated with biotin, avidin/HRP, and 3,3′-diaminobenzidine substrate. Foxm1 expression is increased in a subset of lung adenocarcinomas (*top right* and *middle right*) and squamous cell carcinomas (*bottom right*) compared with corresponding adjacent normal lung tissues (*middle left* and *bottom left*). *Top left,* control for Foxm1 immunostaining, which includes adjacent adenocarcinoma section stained at similar conditions but without first antibody. *D,* Foxm1 and PCNA are coexpressed in human NSCLC. Adjacent paraffin sections of the tissue array were stained with antibodies specific to Foxm1 or PCNA proteins. PCNA expression in human NSCLC was detected by anti-mouse antibody conjugated with alkaline phosphatase and 5-bromo-4-chloro-3-indolyl phosphate/nitroblue tetrazolium substrate. Slides were then counterstained with Nuclear Fast Red. Increased expression of Foxm1 in lung adenocarcinoma and squamous cell carcinoma (*bottom*) is associated with strong PCNA staining in the same lung tumor (*top*). The arrows in *C* and *D* indicate margins of the lung tumor (*Tu*). Magnification: ×100 (*D*); ×200 (*C, bottom* and *middle right*); ×50 (remaining C panels).

compared with *Foxm1* fl/fl mice or Mx-Cre *Foxm1* fl/fl mice treated with PBS (Fig. 3*C*). Interestingly, no large lung adenomas >1 mm in size were found in dsRNA-treated Mx-Cre *Foxm1*$^{-/-}$ lungs, and they displayed a 60% reduction in medium-sized lung adenomas (0.5-1 mm) compared with control mouse lungs (Fig. 3*D*). These results suggest that conditional deletion of *Foxm1* fl/fl allele was sufficient to cause a statistically significant decrease in the number and size of lung adenomas following the urethane tumor induction.

Foxm1 is expressed in pulmonary epithelial cells and lung cancer cells after urethane treatment. Although Foxm1 is not expressed in untreated mouse lungs (Fig. 4*B*; refs. 17, 30), Foxm1 protein was detected in bronchial and alveolar epithelial cells of the urethane-treated *Foxm1* fl/fl mice using immunohistochemical staining with antibody specific for the Foxm1 protein (Fig. 4*B*). Abundant Foxm1 nuclear staining was also detected in all lung tumors of control *Foxm1* fl/fl and PBS-treated Mx-Cre *Foxm1* fl/fl mice (Fig. 4*B*; data not shown). Consistent with RT-PCR analysis (Fig. 3*A* and *B*), dsRNA-treated Mx-Cre *Foxm1*$^{-/-}$ mice displayed a significant reduction of nuclear Foxm1 levels in pulmonary epithelial cells after urethane tumor induction (Fig. 4*B*). Interestingly, 84% of lung tumors in dsRNA-treated Mx-Cre *Foxm1*$^{-/-}$ mice exhibited strong Foxm1 nuclear staining, which was indistinguishable from control *Foxm1* fl/fl tumors (Foxm1-positive tumors; Fig. 4*C*). These results suggest that the majority of lung tumors from dsRNA-treated Mx-Cre *Foxm1*$^{-/-}$ mice resulted from incomplete deletion of the *Foxm1* fl/fl–targeted allele by the Mx-Cre transgene. Only 16% of lung tumors in dsRNA-treated Mx-Cre *Foxm1*$^{-/-}$ mice displayed undetectable Foxm1 levels (Foxm1-negative tumors; Fig. 4*C*), and these Mx-Cre *Foxm1*$^{-/-}$ lung tumors were significantly smaller in size (data not shown), indicating that the Foxm1 induces the growth of lung tumors.

DNA replication is increased in lung tumors expressing the Foxm1. To determine the role of Foxm1 in tumor growth,

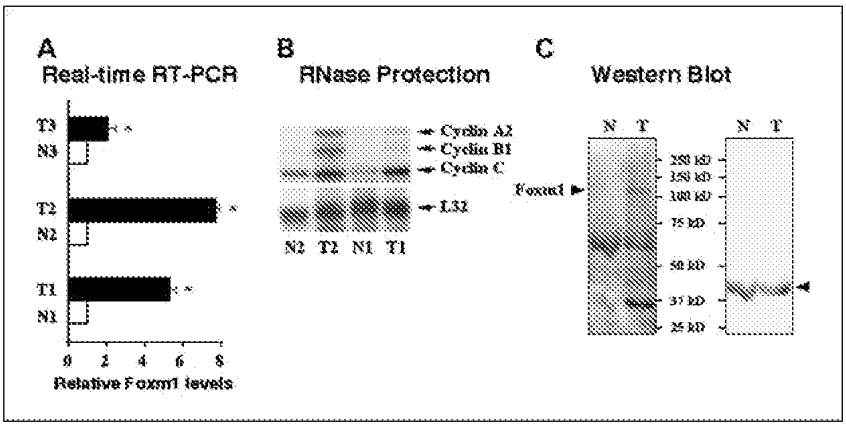

Figure 2. Increased Foxm1 expression in human NSCLC is associated with elevated levels of cyclin A2 and cyclin B1. *A,* real-time RT-PCR analysis confirms increased Foxm1 expression in human NSCLC. Total RNA was prepared from human NSCLC (*T*) and adjacent normal tissues (*N*) and examined for Foxm1 levels by the real-time RT-PCR as described in Materials and Methods. Foxm1 expression levels were normalized to cyclophilin and presented as a fold increase relative to corresponding normal tissue. *, $P < 0.05$, statistical significant differences. *B,* increased Foxm1 levels in human NSCLC are associated with elevated levels of cyclin A2 and cyclin B1. RNase protection assays were done to analyze for expression levels of cyclin mRNA and ribosomal L32 protein using the PharMingen Cyclin RNase protection probes as described previously (17). *C,* Foxm1 protein expression is induced in human NSCLC tumors. Total protein was prepared from normal human lung tissue (*N*) and human lung adenocarcinoma (*T*) and analyzed for Foxm1 and β-actin proteins by Western blot analysis.

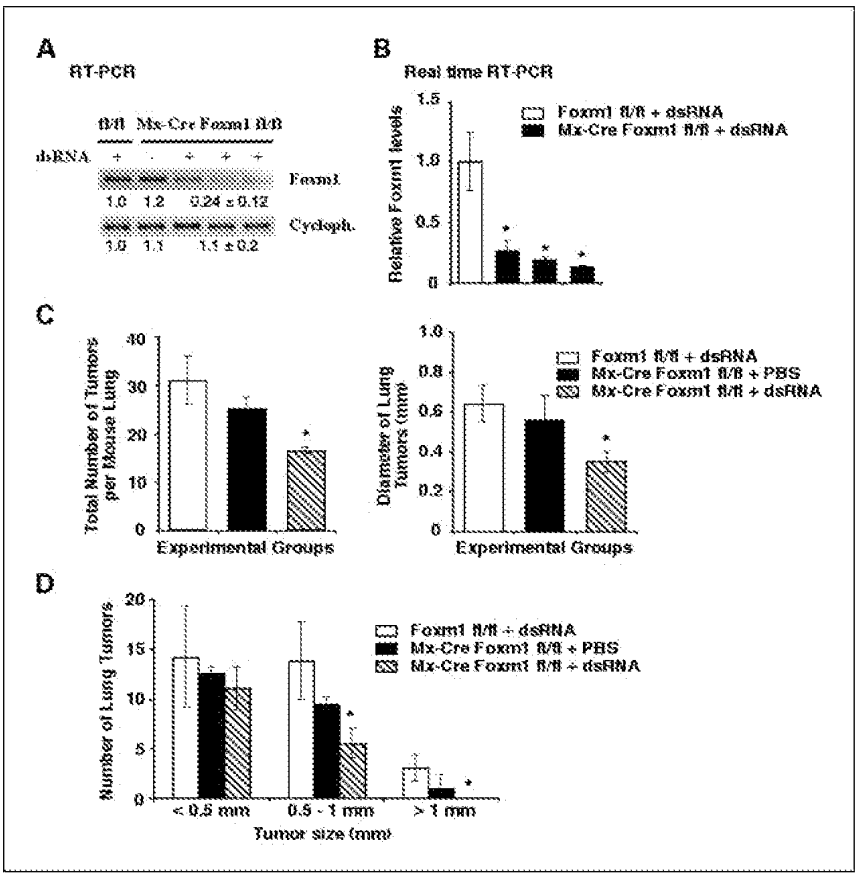

Figure 3. Ubiquitous deletion of Foxm1 decreases the total number and size of urethane-induced lung tumors. Mx-Cre Foxm1 fl/fl and Foxm1 fl/fl mice were injected with dsRNA to activate Cre expression and then subjected to multiple urethane injections to induce lung tumors as described in Materials and Methods. Mx-Cre Foxm1 fl/fl mice, injected with PBS instead of dsRNA, were used as a control. Lungs were dissected and examined for lung tumors and then fixed and paraffin embedded, or used for preparation of total lung RNA. *A-B,* activation of Mx-Cre transgene causes incomplete deletion of Foxm1 fl/fl allele in the lung after urethane tumor induction. Semiquantitative RT-PCR analysis (*A*) and quantitative real-time RT-PCR (*B*) were done with different sets of primers specific to mouse Foxm1 and cyclophilin. Each individual sample was normalized to its corresponding cyclophilin level. *Numbers in A,* means ± SD with respect to *Foxm1* fl/fl mice treated with dsRNA. *C-D,* diminished number and size of lung tumors in Foxm1-deficient mice. Lung tumors from Mx-Cre *Foxm1* fl/fl and *Foxm1* fl/fl mice were counted and measured using a dissecting microscope. Deletion of *Foxm1* fl/fl allele caused a significant reduction (*, $P < 0.05$) in the tumor diameter (*C, right*) and the total number of lung tumors (*C, left*) as well as diminished numbers of large (>1 mm) and medium sized (0.5-1 mm) lung tumors (*D*). Columns, means of the tumor number and tumor diameter using six mouse lungs in each group; *bars,* SD.

we compared DNA replication rates in Foxm1-positive and Foxm1-negative lung tumors in dsRNA-treated Mx-Cre *Foxm1*$^{-/-}$ mice. DNA replication was determined by immunohistochemical detection of BrdUrd that had been administered in drinking water 4 days before sacrificing the mice (12, 29). Foxm1-negative lung tumors from dsRNA-treated Mx-Cre *Foxm1*$^{-/-}$ mice exhibited a significant reduction in DNA replication compared with either control lung tumors or lung tumors from dsRNA-treated Mx-Cre *Foxm1*$^{-/-}$ mice that stain positive for Foxm1 protein (Fig. 4*C* and *D*). These studies provide further evidence that increased Foxm1 expression is associated with high DNA replication rates of lung tumor cells.

Foxm1 deficiency causes reduced expression of cyclin A2 and cyclin B1 in A549 lung adenocarcinoma cells. To determine the role of Foxm1 in the proliferation of A549 human lung adenocarcinoma cells, we transfected these cells with siRNA duplex specific to the human Foxm1 cDNA (siFoxm1) or with mutant control siFoxm1 duplex. Total RNA was prepared 72 hours after siRNA transfection and then analyzed for Foxm1 or cyclin B1 levels by RT-PCR (Fig. 5*A*). These transfection studies revealed that siFoxm1 efficiently reduced the expression of human Foxm1 and its known transcriptional target cyclin B1 (34, 35), whereas transfection of mutant siFoxm1 duplex did not influence expression levels of these genes (Fig. 5*A*). Quantitative real-time RT-PCR confirmed that transfection of siFoxm1 duplex efficiently depleted expression of Foxm1 in A549 cells (Fig. 5*B*).

We next did RNase protection assays to examine temporal expression of the cyclin genes in A549 cells transfected with siFoxm1. Compared with either untransfected cells or cells transfected with mutant siFoxm1, depletion of Foxm1 levels by siFoxm1 caused significant decreases in expression of S phase–promoting *cyclin A2* and M phase–promoting *cyclin B1* genes (Fig. 5*C* and *D*), which is consistent with increased levels of these genes in human adenocarcinoma tumors (Fig. 2*B*). Interestingly, expression levels of cyclin C and cyclin D1 were not affected by siFoxm1 transfection (Fig. 5*C* and *D*). Taken together, our data suggest that Foxm1 selectively activates distinct cyclin genes that promote both S-phase progression and entry into the M-phase of the cell cycle.

Foxm1 stimulates DNA replication and mitosis of lung tumor cells *in vitro*. To determine the role of Foxm1 in DNA replication, A549 cells were transfected with either siFoxm1 or mutant siFoxm1 duplexes or were left untransfected. Seventy-two hours later, cells were pulse labeled for 2 hours with BrdUrd and then fixed and used for immunofluorescent staining with BrdUrd antibody. Depletion of Foxm1 caused a 70% reduction in the number of A549 cells undergoing DNA replication compared with either untransfected A549 cells or cells transfected with mutant siFoxm1 duplex (Fig. 6*A* and *B*). Furthermore, a significant reduction in the number of cells undergoing mitosis were found in siFoxm1-transfected A549 cells as determined by the number of mitotic figures in 4′,6-diamidino-2-phenylindole–stained A549 cell cultures (Fig. 6*B*). These results suggest that depletion of Foxm1 levels inhibit both DNA replication and mitosis in A549 lung adenocarcinoma cells.

Foxm1 deficiency reduces anchorage-independent growth of A549 lung adenocarcinoma cells on soft agar. To examine whether depletion of Foxm1 levels by siRNA transfection would

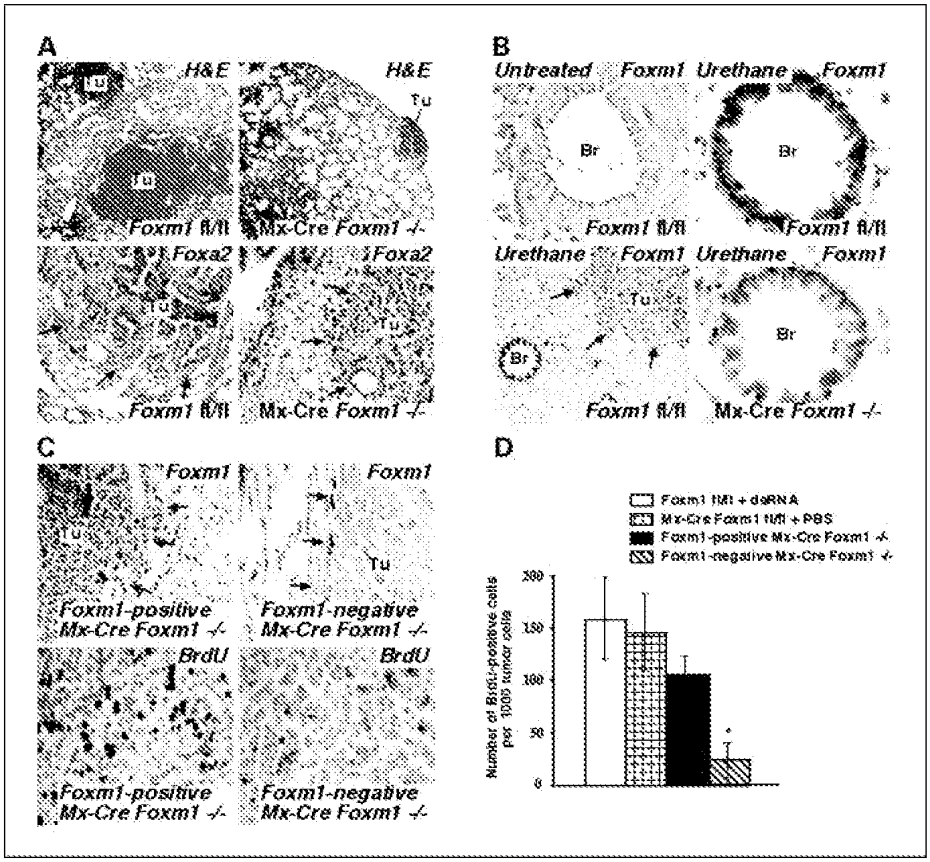

Figure 4. High levels of Foxm1 protein in lung tumors are associated with tumor cell proliferation. Mx-Cre *Foxm1* fl/fl mice were injected with dsRNA to activate Cre expression (Mx-Cre *Foxm1*$^{-/-}$ mice) and then subjected to multiple urethane injections to induce lung tumors. PBS-treated Mx-Cre *Foxm1* fl/fl mice and dsRNA-treated *Foxm1* fl/fl mice were used as controls. Lungs were harvested 28 weeks after initial urethane injection and then fixed and embedded into paraffin blocks. *A,* H&E staining shows a reduction in the size of lung adenomas in Mx-Cre *Foxm1*$^{-/-}$ mice (*top*). Lung paraffin sections were also stained with epithelial-specific Foxa2 antibody to show that lung adenomas in both Mx-Cre *Foxm1*$^{-/-}$ and *Foxm1* fl/fl mice were epithelial in origin (*bottom*). The arrows indicate margins of lung tumor (*Tu*). *B,* Foxm1 expression is induced in lung epithelial cells and lung adenomas after urethane tumor induction. dsRNA-treated mice were subjected to urethane tumor induction protocol. Lung sections from Mx-Cre *Foxm1*$^{-/-}$ and *Foxm1* fl/fl mice were stained with Foxm1 antibody followed by the secondary antibody conjugated with biotin, avidin/HRP, and 3,3′-diaminobenzidine substrate. The Foxm1 protein was not detected in lungs from *Foxm1* fl/fl mice without urethane tumor induction (*top left*). Abundant Foxm1 nuclear staining was observed in bronchial epithelial cells (*Br*) and tumor cells (*Tu*) in urethane-treated *Foxm1* fl/fl lungs (*top right* and *bottom left*). Mx-Cre *Foxm1*$^{-/-}$ lungs display reduced Foxm1 staining in bronchial epithelium (*bottom right*). *C-D,* diminished DNA replication in Foxm1-negative lung tumors of Mx-Cre *Foxm1*$^{-/-}$ mice. Adjacent paraffin sections from Mx-Cre *Foxm1*$^{-/-}$ lungs were stained with Foxm1 antibody (*C, top*) or BrdUrd antibody (*C, bottom*). We counted BrdUrd-positive cells per 1,000 tumor cells in 10 distinct Foxm1-positive or Foxm1-negative Mx-Cre *Foxm1*$^{-/-}$ lung tumors (*D*). Tumors from dsRNA-treated *Foxm1* fl/fl and PBS-treated Mx-Cre *Foxm1* fl/fl mice were used as controls (*D*). Three mice were used in each group. *, $P < 0.05$. Magnification: ×50 (*A, top*); ×100 (*B, bottom left*); 200× (*A, bottom* and *C, top*); ×400 (the rest).

inhibit anchorage-independent growth of the lung tumor cells on soft agar, A549 cells were transfected separately with siFoxm1 or mutant siFoxm1 duplexes or left untransfected. One day later, cells were plated on soft agar for 2 weeks. Depletion of Foxm1 levels by siRNA dramatically reduced anchorage-independent growth, as evidenced by the significant decrease in the number of A549 cell colonies on soft agar (Fig. 6*C* and *D*). In contrast, transfection of the mutant siFoxm1 duplex into A549 cells did not affect the number of A549 cell colonies growing on soft agar (Fig. 6*C* and *D*). These results suggest that depletion of Foxm1 expression by siRNA transfection reduces oncogenic properties of A549 lung adenocarcinoma cells by reducing anchorage-independent growth of cell colonies on soft agar.

Discussion

Transgenic and gene knockout mouse studies showed that Foxm1 is critical for DNA replication and is essential for mitotic progression (10, 11, 13, 14, 17, 35–37). Consistent with the important role of Foxm1 in cell cycle progression, elevated Foxm1 levels have been found in numerous cell lines derived from human tumors (18–20). Increased expression of Foxm1 protein was also found in variety of human tumors, including hepatocellular carcinoma (26), basal cell carcinoma (21), breast adenocarcinoma (24), astrocytoma, and glioblastoma (23), suggesting that the Foxm1 regulates cellular proliferation in various human cancers. Mice with hepatocyte-specific deletion of *Foxm1* fl/fl allele exhibit defects in hepatocyte proliferation and fail to develop hepatocellular carcinoma in response to a diethylnitrosamine/phenobarbital liver tumor induction protocol (12). In this study, we investigated the role of Foxm1 in NSCLC using the mouse experimental model of lung tumorigenesis, as well as human NSCLC tumors.

We showed that Foxm1 and PCNA proteins are coexpressed in a subset of human NSCLC tumors. Interestingly, virtually undetectable PCNA staining was found in NSCLC tumors with low levels of Foxm1 protein (data not shown), suggesting that

Foxm1 expression is induced in human NSCLC undergoing rapid proliferation. Alternatively, the absence of Foxm1 in subset of lung cancers can be explained by poor preservation of lung tissue during collection of some human samples. Furthermore, immunohistochemistry with Foxm1 antibody displayed both nuclear and cytoplasmic staining in human lung tumors. Because the Foxm1 antibody recognized several proteins with lower than Foxm1 molecular weight in human adenocarcinoma tissue (Western blot in Fig. 2*C*), this cytoplasmic staining may include nonspecific immunoreactivity or products of Foxm1 degradation.

We found that the Mx-Cre transgene caused the deletion of *Foxm1* fl/fl–targeted allele in 75% of Mx-Cre *Foxm1*$^{-/-}$ pulmonary cells, yet this was sufficient to cause a statistically significant reduction in the number and size of lung adenomas. Interestingly, ~84% of lung tumors in Mx-Cre *Foxm1*$^{-/-}$ mice exhibited strong Foxm1 nuclear staining, indicating that the majority of Mx-Cre *Foxm1*$^{-/-}$ lung tumors resulted from incomplete deletion of *Foxm1* fl/fl–targeted allele by the Mx-Cre transgene. Undetectable Foxm1 expression was observed only in 16% of Mx-Cre *Foxm1*$^{-/-}$ lung tumors, which exhibited reduced BrdUrd incorporation and tumor size. These results strongly suggest that increased expression of Foxm1 correlates with high levels of proliferation and growth of lung tumors. Our results also suggest that lung tumors can arise from *Foxm1*$^{-/-}$ epithelial cells, probably due to secondary mutations that bypass a block in cell cycle progression caused by Foxm1 deficiency.

The Mx-Cre transgene deletes the *Foxm1* fl/fl–targeted allele in a mosaic fashion in all cell types of the lung (27); therefore, the cancer resistance in Mx-Cre *Foxm1*$^{-/-}$ mice can be explained by the direct Foxm1 effect on proliferation of epithelial-derived tumor cells, or by effects of Foxm1 deletion on tumor angiogenesis. This is consistent with our previous report showing that Foxm1 is essential for proliferation of pulmonary endothelial cells during lung embryonic development (14). However, we were unable to detect significant differences in either the morphologic appearance of pulmonary endothelial cells or the expression levels of endothelial-specific Pecam-1 protein in *Foxm1* fl/fl and Mx-Cre *Foxm1*$^{-/-}$ lungs (data not shown). Because *Foxm1*$^{-/-}$ tumor cells displayed diminished BrdUrd incorporation, we used siRNA specific to Foxm1 to investigate the direct effects of Foxm1 on the proliferation of A549 human lung adenocarcinoma cells. These transfection studies revealed that depletion of Foxm1 levels efficiently inhibited both DNA replication and mitosis in this lung tumor cell line. These results are also consistent with our previous studies that transgenic overexpression of Foxm1 accelerates the onset of DNA replication and mitosis in mouse lungs following BHT-mediated lung injury (17).

It is interesting to note that the *Foxm1* fl/fl–targeted allele was deleted before the urethane tumor induction in Mx-Cre *Foxm1*$^{-/-}$ mice; therefore, the Foxm1 deletion occurred before the tumor initiation in Mx-Cre *Foxm1*$^{-/-}$ mice. Because Mx-Cre *Foxm1*$^{-/-}$ lungs displayed a significant reduction in total number of lung adenomas, Foxm1 may induce the initiation of NSCLC cancer

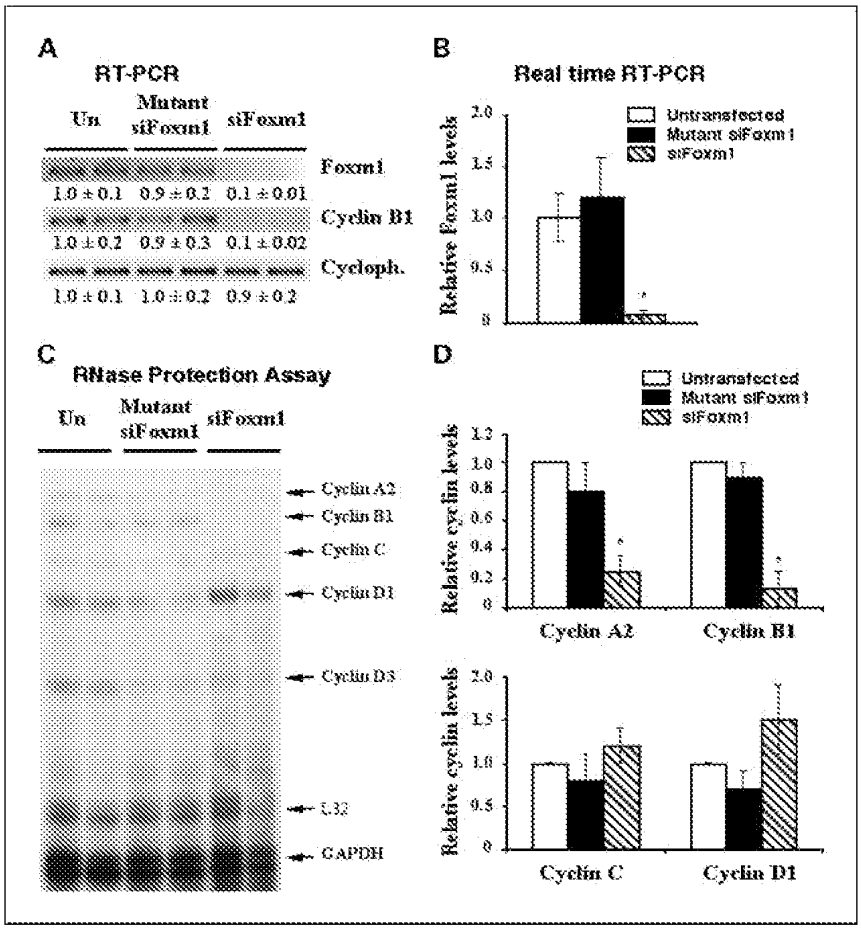

Figure 5. Foxm1 deficiency causes reduced expression of cyclin A2 and cyclin B1. We transfected either siFoxm1 or mutant siFoxm1 duplexes into A549 cells. After 72 hours, transfected A549 cells were used for preparation of total RNA. *A-B,* transfection of siFoxm1 inhibits expression of Foxm1 and its target gene *cyclin B1* in A549 cells. Total RNA was analyzed for expression levels of Foxm1, cyclin B1, and cyclophilin by the semiquantitative RT-PCR analysis (*A*) and quantitative real-time RT-PCR (*B*). Each individual sample was normalized to its corresponding cyclophilin level. *Numbers in A,* means ± SD with respect to untransfected (*Un*) A549 cells. *, $P < 0.05$. *C-D,* depletion of Foxm1 reduces the expression of cyclin A2 and cyclin B1. RNase protection assays (*C*) were used to analyze for expression levels of cyclin mRNA with the PharMingen Cyclin RNase protection probes as described previously (17). Cyclin levels were normalized to glyceraldehyde-3-phosphate dehydrogenase (*GAPDH*) mRNA levels, and expression levels were presented with respect to untransfected (*Un*) cells (*D*).

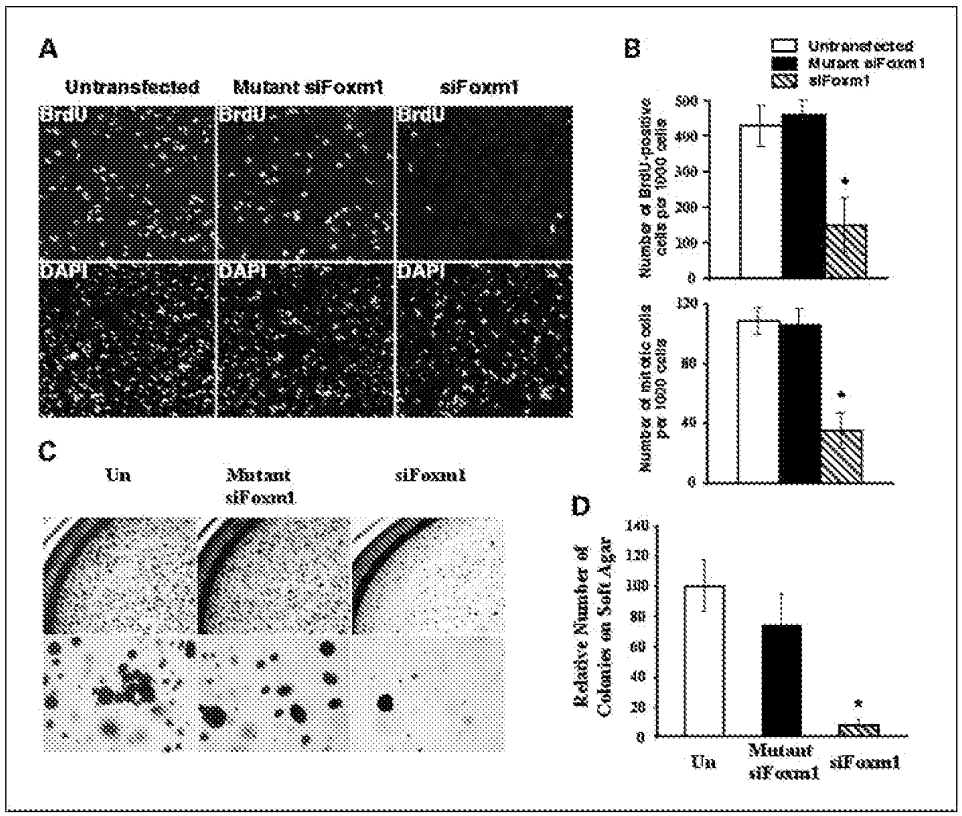

Figure 6. Depletion of Foxm1 reduces proliferation of A549 adenocarcinoma cells and inhibits the anchorage-independent growth of these cells on soft agar. *A-B*, siFoxm1 transfection diminishes the total number of cells undergoing DNA synthesis and mitosis. A549 cells transfected with either siFoxm1 or mutant siFoxm1 were treated with BrdUrd for 2 hours and then fixed and immunostained with mouse monoclonal antibodies specific for BrdUrd followed by anti-mouse antibody conjugated with FITC (*A, top*). Cell nuclei were counterstained with 4′,6-diamidino-2-phenylindole (*A, bottom*). We counted the number of BrdUrd-positive cells (*B, top*) as well as mitotic figures in five random microscope fields (*B, bottom*). *Columns*, mean percentage of cells (three distinct transfections); *bars*, SD. *, $P < 0.05$. *C-D*, siFoxm1 transfection diminishes anchorage-independent growth of A549 lung adenocarcinoma cells on soft agar. A549 cells were left untransfected (*Un*) or transfected with 100 nmol/L of either siFoxm1 or mutFoxm1. One day after transfection, the cells were trypsinized and plated on soft agar for 2 weeks to assay for anchorage-independent cell growth as described previously (12). *Columns*, mean number of colonies relative to untransfected cultures (triplicate plates were used to count colonies); *bars*, SD (*D*). *, $P < 0.01$.

in vivo. Further support for this concept is provided by the *in vitro* colony formation assay showing that depletion of Foxm1 levels by siRNA dramatically reduced the ability of A549 cells to form colonies on soft agar. This finding is consistent with our previous studies showing that induced Foxm1 expression stimulated U2OS cells to form colonies on soft agar and use of a membrane penetrating $(D\text{-}Arg)_9$-ARF 26-44 peptide inhibitor of Foxm1 prevented U2OS cells to form colonies on soft agar (12). Furthermore, our data clearly indicate that urethane treatment induces Foxm1 expression in both lung tumor cells and normal bronchial epithelial cells. These results suggest that overexpression of the Foxm1 in normal bronchial cells is not sufficient to induce aberrant proliferation. Abundant Foxm1 expression in urethane-induced epithelial cells may prevent the use of this protein as a marker for lung cancer diagnosis. However, because our results clearly show that deletion of Foxm1 decreases both incidence and growth of urethane-induced lung tumors, Foxm1 may represent a new therapeutic target to inhibit the tumor progression.

Progression into the S phase requires activation of Cdk2 in complex with either cyclin E or cyclin A2, which cooperates with cyclin D-cdk4/cdk6 to phosphorylate the retinoblastoma protein. This releases a bound E2F transcription factor and allows it to stimulate expression of genes required for DNA replication (38, 39). Here, we found that Foxm1 deficiency was associated with reduced cyclin A2 levels and therefore contributes to diminished DNA replication in Foxm1-depleted A549 cells. Foxm1-deficient cells also displayed reduced expression of *cyclin B1*, a known Foxm1 target gene (34, 35), which activates cdk1 during cellular progression into the M phase (40). Our results are also consistent with premature expression of the cyclin A2 and cyclin B1 during lung injury in Rosa26-Foxm1 transgenic mice (17). These data suggest that Foxm1 directly regulates distinct pulmonary pathways that promote both S-phase progression and entry into the M phase during the progression of lung cancer. Furthermore, recent studies have shown that increased cyclin A2 level is responsible for c-Jun transcription factor to induce growth of Rat1A cells on soft agar (41). The fact that depletion of Foxm1 significantly reduces expression of cyclin A2 suggests that diminished cyclin A2 levels in Foxm1-depleted A549 cells contribute to reduced anchorage-independent growth on soft agar.

In summary, Foxm1 is abundantly expressed in urethane-induced lung cancer from adult mice as well as in highly proliferative human NSCLC tumors. Induced expression of the Mx-Cre recombinase transgene resulted in conditional deletion of *Foxm1* fl/fl–targeted allele causing significant reduction in the proliferation of lung tumor cells as well as in number and size of lung adenomas following urethane treatment. Depletion of Foxm1 expression by siRNA transfection of A549 lung adenocarcinoma cells caused significant decreases in DNA replication and mitosis and reduced anchorage-independent growth of cell colonies on soft agar, showing that Foxm1 directly stimulates the proliferation of lung tumor cells during development of NSCLC.

Acknowledgments

Received 8/23/2005; revised 11/16/2005; accepted 12/8/2005.

Grant support: American Cancer Society, Illinois Division research grant 06-09 (V.V. Kalinichenko); American Heart Association Scientist Development grant 0335036N (V.V. Kalinichenko); and National Institutes of Diabetes, Digestive and Kidney Diseases/USPHS grant DK 54687-06 (R.H. Costa).

The costs of publication of this article were defrayed in part by the payment of page charges. This article must therefore be hereby marked *advertisement* in accordance with 18 U.S.C. Section 1734 solely to indicate this fact.

References

1. Kerr KM. Pulmonary preinvasive neoplasia. J Clin Pathol 2001;54:257–71.
2. McCormick F. Signalling networks that cause cancer. Trends Cell Biol 1999;9:M53–6.
3. Sherr CJ, McCormick F. The RB and p53 pathways in cancer. Cancer Cell 2002;2:103–12.
4. Malkinson AM. Molecular comparison of human and mouse pulmonary adenocarcinomas. Exp Lung Res 1998;24:541–55.
5. Giaccone G. Oncogenes and antioncogenes in lung tumorigenesis. Chest 1996;109:130–4S.
6. Mitsuuchi Y, Testa JR. Cytogenetics and molecular genetics of lung cancer. Am J Med Genet 2002;115:183–8.
7. Major ML, Lepe R, Costa RH. Forkhead box M1B (FoxM1B) transcriptional activity requires binding of Cdk/cyclin complexes for phosphorylation-dependent recruitment of p300/CBP co-activators. Mol Cell Biol 2004;24:2649–61.
8. Ma RY, Tong TH, Cheung AM, Tsang AC, Leung WY, Yao KM. Raf/MEK/MAPK signaling stimulates the nuclear translocation and transactivating activity of FOXM1c. J Cell Sci 2005;118:795–806.
9. Costa RH, Kalinichenko VV, Major ML, Raychaudhuri P. New and unexpected: forkhead meets ARF. Curr Opin Genet Dev 2005;15:42–8.
10. Wang X, Kiyokawa H, Dennewitz MB, Costa RH. The Forkhead box m1b transcription factor is essential for hepatocyte DNA replication and mitosis during mouse liver regeneration. Proc Natl Acad Sci U S A 2002;99:16881–6.
11. Wang X, Krupczak-Hollis K, Tan Y, Dennewitz MB, Adami GR, Costa RH. Increased hepatic Forkhead box M1B (FoxM1B) levels in old-aged mice stimulated liver regeneration through diminished p27Kip1 protein levels and increased Cdc25B expression. J Biol Chem 2002;277:44310–6.
12. Kalinichenko VV, Major M, Wang X, et al. Forkhead Box m1b transcription factor is essential for development of hepatocellular carcinomas and is negatively regulated by the p19ARF tumor suppressor. Genes Development 2004;18:830–50.
13. Krupczak-Hollis K, Wang X, Kalinichenko VV, et al. The mouse Forkhead Box m1 transcription factor is essential for hepatoblast mitosis and development of intrahepatic bile ducts and vessels during liver morphogenesis. Dev Biol 2004;276:74–88.
14. Kim IM, Ramakrishna S, Gusarova GA, Yoder HM, Costa RH, Kalinichenko VV. The forkhead box M1 transcription factor is essential for embryonic development of pulmonary vasculature. J Biol Chem 2005;280:22278–86.
15. Glover DM, Hagan IM, Tavares AA. Polo-like kinases: a team that plays throughout mitosis. Genes Dev 1998;12:3777–87.
16. Adams RR, Carmena M, Earnshaw WC. Chromosomal passengers and the (aurora) ABCs of mitosis. Trends Cell Biol 2001;11:49–54.
17. Kalinichenko VV, Gusarova GA, Tan Y, et al. Ubiquitous expression of the forkhead box M1B transgene accelerates proliferation of distinct pulmonary cell-types following lung injury. J Biol Chem 2003;278:37888–94.
18. Korver W, Roose J, Clevers H. The winged-helix transcription factor Trident is expressed in cycling cells. Nucleic Acids Res 1997;25:1715–9.
19. Yao KM, Sha M, Lu Z, Wong GG. Molecular analysis of a novel winged helix protein, WIN. Expression pattern, DNA binding property, and alternative splicing within the DNA binding domain. J Biol Chem 1997;272:19827–36.
20. Ye H, Kelly TF, Samadani U, et al. Hepatocyte nuclear factor 3/fork head homolog 11 is expressed in proliferating epithelial and mesenchymal cells of embryonic and adult tissues. Mol Cell Biol 1997;17:1626–41.
21. Teh MT, Wong ST, Neill GW, Ghali LR, Philpott MP, Quinn AG. FOXM1 is a downstream target of Gli1 in basal cell carcinomas. Cancer Res 2002;62:4773–80.
22. Obama K, Ura K, Li M, et al. Genome-wide analysis of gene expression in human intrahepatic cholangiocarcinoma. Hepatology 2005;41:1339–48.
23. van den Boom J, Wolter M, Kuick R, et al. Characterization of gene expression profiles associated with glioma progression using oligonucleotide-based microarray analysis and real-time reverse transcription-polymerase chain reaction. Am J Pathol 2003;163:1033–43.
24. Wonsey DR, Follettie MT. Loss of the forkhead transcription factor FoxM1 causes centrosome amplification and mitotic catastrophe. Cancer Res 2005;65:5181–9.
25. Pilarsky C, Wenzig M, Specht T, Saeger HD, Grutzmann R. Identification and validation of commonly overexpressed genes in solid tumors by comparison of microarray data. Neoplasia 2004;6:744–50.
26. Lee JS, Chu IS, Heo J, et al. Classification and prediction of survival in hepatocellular carcinoma by gene expression profiling. Hepatology 2004;40:667–76.
27. Kuhn R, Schwenk F, Aguet M, Rajewsky K. Inducible gene targeting in mice. Science 1995;269:1427–9.
28. Miller YE, Dwyer-Nield LD, Keith RL, Le M, Franklin WA, Malkinson AM. Induction of a high incidence of lung tumors in C57BL/6 mice with multiple ethyl carbamate injections. Cancer Lett 2003;198:139–44.
29. Ledda-Columbano GM, Pibiri M, Concas D, Cossu C, Tripodi M, Columbano A. Loss of cyclin D1 does not inhibit the proliferative response of mouse liver to mitogenic stimuli. Hepatology 2002;36:1098–105.
30. Kalinichenko VV, Lim L, Shin B, Costa RH. Differential expression of Forkhead box transcription factors following butylated hydroxytoluene lung injury. Am J Physiol Lung Cell Mol Physiol 2001;280:L695–704.
31. Kalinichenko VV, Lim L, Beer-Stoltz D, et al. Defects in pulmonary vasculature and perinatal lung hemorrhage in mice heterozygous null for the Forkhead box f1 transcription factor. Dev Biol 2001;235:489–506.
32. Kalinichenko VV, Zhou Y, Bhattacharyya D, et al. Haploinsufficiency of the mouse Forkhead box f1 gene causes defects in gall bladder development. J Biol Chem 2002;277:12369–74.
33. Stahlman MT, Gray ME, Whitsett JA. Temporal-spatial distribution of hepatocyte nuclear factor-3beta in developing human lung and other foregut derivatives. J Histochem Cytochem 1998;46:955–62.
34. Leung TW, Lin SS, Tsang AC, et al. Over-expression of FoxM1 stimulates cyclin B1 expression. FEBS Lett 2001;507:59–66.
35. Wang X, Quail E, Hung N-J, Tan Y, Ye H, Costa RH. Increased levels of Forkhead box M1B transcription factor in transgenic mouse hepatocytes prevents age-related proliferation defects in regenerating liver. Proc Natl Acad Sci U S A 2001;98:11468–73.
36. Korver W, Schilham MW, Moerer P, et al. Uncoupling of S phase and mitosis in cardiomyocytes and hepatocytes lacking the winged-helix transcription factor trident. Curr Biol 1998;8:1327–30.
37. Ye H, Holterman A, Yoo KW, Franks RR, Costa RH. Premature expression of the winged helix transcription factor HFH-11B in regenerating mouse liver accelerates hepatocyte entry into S-phase. Mol Cell Biol 1999;19:8570–80.
38. Harbour JW, Dean DC. The Rb/E2F pathway: expanding roles and emerging paradigms. Genes Dev 2000;14:2393–409.
39. Ishida S, Huang E, Zuzan H, et al. Role for E2F in control of both DNA replication and mitotic functions as revealed from DNA microarray analysis. Mol Cell Biol 2001;21:4684–99.
40. Nilsson I, Hoffmann I. Cell cycle regulation by the Cdc25 phosphatase family. Prog Cell Cycle Res 2000;4:107–14.
41. Katabami M, Donninger H, Hommura F, et al. Cyclin A is a c-Jun target gene and is necessary for c-Jun-induced anchorage-independent growth in RAT1a cells. J Biol Chem 2005;280:16728–38.